Anal Bioanal Chem (2008) 391:1813–1820
DOI 10.1007/s00216-008-2022-z

ORIGINAL PAPER

Colloidal-based localized surface plasmon resonance (LSPR) biosensor for the quantitative determination of stanozolol

Mark P. Kreuzer · Romain Quidant · J.-Pablo Salvador · M.-Pilar Marco · Gonçal Badenes

Received: 21 November 2007 / Revised: 13 February 2008 / Accepted: 22 February 2008 / Published online: 30 March 2008

Abstract This work reports the systematic preparation of biosensors through the use of functionalized glass substrates, noble metal gold colloid, and measurement by localized surface plasmon resonance (LSPR). Glass substrate was modified through chemical silanization, and the density of gold colloid was carefully controlled by optimizing the conditions of silanization through the use of mixed silanes and selective mixing procedures. At this point, samples were exposed to bioreagents and changes in the shallow dielectric constant around the particles were observed by dark-field spectroscopy. Biological binding of high affinity systems (biotin/streptavidin and antigen/antibody) was subsequently investigated by optimizing coating layers, receptor concentration profiling, and finally quantitative determination of the analyte of interest, which in this case was a small organic molecule—the widely used, synthetic anabolic steroid called stanozolol. For this system, high specificity was achieved (>97%) through extensive nonspecific binding tests, with a sensitivity measurable to a level below the minimum required performance level (MRPL) as determined by standard chromatographic methods. Analytical best-fit parameters of Hillslope and regression coefficient are also commented on for the final LSPR biosensor. The LSPR biosensor showed good reproducibility (<5% RSD) and allowed for rapid preparation of calibration curves and determination of the analyte (measurement time of each sample ca. 2 min). As an alternative method for quantitative steroidal analysis, this approach significantly simplifies the detection setup while reducing the cost of analysis. In addition the system maintains comparable sensitivity to standard surface plasmon resonance methods and offers great potential for miniaturization and development of multiplexed devices.

Keywords Localized surface plasmon resonance · Stanozolol · Colloid · Nanoparticles · Biosensor

Introduction

Biosensing by surface plasmon resonance (SPR) was first established in the early 1980s and quickly became the benchmark technique for unlabelled sensing over the following 25 years. The method takes advantage of the local change of the dielectric function at the surface of an extended flat-film gold layer to which the biological compounds have been immobilized. Changes in the phase angle are then measured when the appropriate ligand subsequently bind. Because of the flat gold film structure, it represents a two-dimensional arrangement for the detection of the biomolecules. In more recent times, progress in SPR development has slowed with interest in pushing the limits of detection even further. One important realization was that incorporating labels (largely, metallic particles) gave rise to substantial changes in the evanescent environment close to the metal–dielectric junction that led to an enhancement factor when

Electronic supplementary material The online version of this article (doi:10.1007/s00216-008-2022-z) contains supplementary material, which is available to authorized users.

M. P. Kreuzer (✉) · R. Quidant · G. Badenes
ICFO Institute of Photonic Science,
Mediterranean Technology Park,
08860 Castelldefels, Spain
e-mail: mark.kreuzer@icfo.es

J.-P. Salvador · M.-P. Marco
Department of Biological Organic Chemistry, CSIC,
Jordi Girona 18–26,
08034 Barcelona, Spain

biological molecules bore these metal labels [1–3]. In essence the presence of metallic particles greatly changed the immediate environment close to the sensing surface leading to much larger phase angle shifts than for systems not incorporating them [4–5].

In our case we also use metallic nanoparticles but do not use their intrinsic refractive index to amplify an SPR signal. Instead, with the exclusion of the surface plasmon polariton mode by the absence of the continuous gold layer, we probe the localized fields associated with the nanoparticles and use them to highlight an alternative approach to plasmon sensing, of the localized kind. This type of sensing has recently awakened a large interest for their potentially improved characteristics. Through the three-dimensional arrangement of colloids, the main advantages of localized surface plasmon resonance (LSPR)-based sensors rely on the fact that gold plasmon resonant particles with diameters between 30 and 120 nm efficiently scatter light in the visible spectrum. The particle geometric confinement of the surface plasmon gives rise to a spectral resonance in the light scattering that does not occur in thin films such as those of SPR sensors. Moreover, the smaller active area of the gold and thus the sensing layer (sensor size) and a simplification of the optical setup may contribute to further on-a-chip integration [6] and the development of multianalyte methods. Additionally, under appropriate arrangement, the plasmon mode engineering is expected to offer enhanced sensitivity compared with flat-film SPR [7].

For convenience and easier end-user applicability, we have chosen to work with signals detected by a number of separated colloidal gold nanoparticles rather than with single nanoparticles. Provided that the particles are separated enough to weakly interact, this allows for measuring a strong signal and thus we can consider the ensemble to respond spectrally in a similar way to an isolated nanoparticle [8]. For this reason, the establishment of a reproducible methodology for the preparation of glass surfaces with nanoparticles homogeneously distributed and covalently immobilized has been crucial.

To demonstrate applicability of this sensing principle for residue analysis, we have employed immunoreagents specifically developed for the detection of stanozolol, an androgenic hormone used illegally as a growth promoter in farm animals and to increase athletic performance. The European Union (EU) has completely prohibited the use of these steroidal hormones for meat production since 1981 (Directive 81/602/EEC), which applies to Member States and imports from third-party countries alike.

Within this report lie the results of extended investigations on the systematic development of an LSPR biosensor. We have endeavored to highlight the advantages of using these noble metal colloids for the development, through analytical means, of a relatively simple system that rapidly, specifically, and with sufficient sensitivity detects anabolic steroids. The key developments are in the relative ease of preparing the sensors (through the use of colloids and mixed surface-assembled monolayers) both from a fabrication and (bio)chemical viewpoint.

Material and methods

Reagents

Aminopropyltrimethoxysilane (APTMS), ethyltrimethoxysilane (ETMS), anti-rabbit IgG coupled to horseradish peroxidase (IgG-HRP), 3,3′,5,5′-tetramethylbenzidine (TMB), hydrogen peroxide (H_2O_2), biotin, and streptavidin were obtained from Sigma-Aldrich (Madrid, Spain). Stanozolol (St) was from Sequoia Research Products (Oxford, UK). All other reagents were of the highest grade available and when required, solvents were distilled prior to use. Derivatives of St (bovine serum albumin (BSA) and horseshoe crab hemocyanin (HSH)) and stanozolol polyclonal antiserum (α-St pAbs) were prepared in-house. Atrazine (At-BSA) was prepared as previously described [9]. Phosphate-buffered saline (PBS) used in the immunochemical methods was 10 mM with 0.001% Tween-20 at pH 7.4. Substrate buffer was 0.04 M citrate buffer, pH 5.5, containing 0.6% TMB and 1% H_2O_2. BK7 glass was purchased from Marienfeld (Lauda-Königshofen, Germany). Gold colloid (100 nm) came from BBInternational (Cardiff, UK).

Stanozolol immunoreagents

Hapten modification, coating, and immunization conjugate preparation (St-BSA and St-HCH) and antiserum development procedures are extensively described in the Electronic supplementary material.

Apparatus

Optical arrangement

The optical setup consisted of a standard BX5 microscope (Olympus, Germany). The extinction spectra of the gold colloids were measured by conventional dark-field spectroscopy. The sample illumination was performed from with halogen lamp (100 W) using an immersion-oil dark-field condenser with high numerical aperture (NA=1.4–1.2). The light scattered by the particles was collected by a long working distance objective lens (×50, NA=0.5) and sent toward both an Ocean Optics microspectrometer (model HR 2000) and a CCD camera (Q-imaging, Spain). An adjustable diaphragm located at the microscope output was used to reduce the detection area to approximately 100 μm^2.

Considering the bandwidth of the particles' extinction spectra, the setup allows for the determination of the central LSPR wavelength with a resolution of ca. 0.3 nm.

Atomic force microscopy

The gold colloid distribution at the substrate surface was characterized by a commercial atomic force microscope (Digital Instrument D3100). Measurements done in tapping mode using a Si cantilever (300 kHz, Veeco, Spain) with a stiffness of 40 N/m allowed us to observe the clustering between the gold colloids when lying at the substrate surface.

Colorimetric determination and data analysis

Absorbance measurements in the visible region were performed using a SpectramaxPlus (Molecular Devices, Sunnyvale, CA). Competitive curves were analyzed with a four-parameter logistic equation using the software SoftmaxPro v2.6 (Molecular Devices) and GraphPad Prism (GraphPad Software Inc., San Diego, CA).

Procedures

Chemical modification of glass substrates

Glass substrate was sonicated for 1 min in ethanol (EtOH) before drying under nitrogen (N_2). The substrate was then activated for 1 h at room temperature (RT) using 2 N sodium hydroxide containing 50% (v/v) EtOH, according to Tätte et al. [10]. After washing thoroughly with water and drying under N_2, either MPTMS in an inert atmosphere (argon and vacuum) or a mixture of APTMS/ETMS in EtOH was applied to one side of the glass for 2 min at RT. After excessive washing with EtOH and water, gold colloid solution was added in 20-μL droplets at RT for a predetermined time. Samples were then washed in MilliQ water and dried under a stream of N_2. These samples were used immediately as described in the following section.

Biological modification of gold colloid

Gold-modified glass substrates were primarily functionalized with biotin, St-BSA, or At-BSA for 30 min at RT. The binding of biotin was done empirically ranging between 0.2 and 1.0 mM. The concentration of St-BSA, henceforth called the coating agent, was optimized in a dose-dependent manner by applying various concentrations (0.01–100 μg/mL in 10 mM PBS at pH 7.4) and measuring the corresponding resonance changes. For specificity studies, which determine whether the sensor is giving signals solely for the correct binding between the coating (capture) agent and the target (analyte of interest) and not through some additional, unwanted binding to the surrounding landscape, an identical concentration of At-BSA was used as it had a similar hapten (analyte) loading and identical spatial volume because of the BSA carrier protein, when compared with St-BSA. After washing with MilliQ water, the scattering spectrum was measured and this constituted the reference spectrum. In addition to this, the spectrum from bare colloid was also measured, prior to addition of biotin or St-BSA as a reference for the first binding. This allows a way to check that there is no spectral broadening from the gold alone. In order to optimize the binding of corresponding receptor, α-St pAbs, dose-dependent curves were prepared by varying the dilution of the pAbs (1:10 to 1:100,000 in 10 mM PBS with 0.001% Tween 20, pH 7.4). This binding lasted 30 min at RT. In the case of streptavidin, we used an arbitrary standard concentration of 1.5 μM. This was deemed sufficient to measure a resonance shift and thus prove the concept of selective binding by the streptavidin receptor. Quantitation of St by LSPR was achieved by preparing different St standards (1–10,000 nM) and mixing with the optimum α-St pAb dilution via two steps. The first was a preincubation of 15 min at RT followed by addition of each mixture to the corresponding St-BSA-coated gold substrates for a further 30 min (20-μL droplets). After washing, scattering curves were recorded for each St concentration and compared with the reference spectrum. The amount of St present in the sample is inversely proportional to the wavelength change determined by standard dose–response curves, constructed by plotting the wavelength against antigen standard concentration.

Nonspecific binding controls measured the degree of binding of α-St pAbs to silanized glass (absence of Au colloid and coating agent St-BSA), to atrazine-BSA and to a BSA-coated gold colloid (BSA without analyte linked). NSB is extensively explained in the Results and discussion.

Colorimetric assessment

Anti-rabbit IgG-HRP (1:6,000 in PBS) was used to assess antibody binding to the St-BSA-derivatized gold particles, and also nonspecific binding occurring with the surface and/or gold colloid itself. This species was incubated, after excessive washing, for 30 min at RT after the α-St pAbs had bound. Through the addition of the TMB substrate solution, the color evolved was measured at 450 nm (see Electronic supplementary material for image of setup).

Results and discussion

As mentioned previously we have chosen to work with an homogeneous distribution of gold colloid with average minimum interparticle distance of 1 μm, as determined by atomic force microscopy (data not shown). Under these

conditions, the particles weakly interact so that we can consider the ensemble responds spectrally in a similar way to an isolated nanoparticle. In practice however this is not so easy to achieve. The arrangement of the colloid in such an organized/dispersed fashion resulted from various permutations. It was paramount that clustering of the particles be avoided and all methods attempted tried to achieve this essential goal.

Optimization of colloid density on glass substrates

This work takes advantage of the characteristic resonance spectrum of gold particles of 100-nm diameter, in which the typical resonance can be seen around at 550 nm and emission of a green color occurs in the dark-field spectrum. Initial experiments, using solely MPTMS as the silanization agent, found that reproducibility of gold binding (density) was poor. Its use warranted close control of the environment to avoid oxidation of the thiol group essential in binding the gold. In contrast, when APTMS was used, the gold binding was similar to MPTMS in terms of density but with no variation in this density over a time period >3 months (under identical conditions). In addition, by using APTMS it was easier to modify the glass, as inert conditions were no longer required (argon and vacuum).

Primarily, APTMS was investigated by varying its concentration in ethanol (34 μM to 1.13 mM), time of contact with the glass substrate, and the judicial mixing with ETMS to avoid clustering. ETMS chemically binds to glass in an identical fashion as APTMS, through its silane functionality, but only exposes an ethyl group ($–CH_2CH_3$) at the other end of the molecule, which is not active for subsequent linking to gold. By using ETMS in a mixed SAM system, it contributes by spacing the active APTMS depending on the ratio used and thus controlling better the position of the gold colloid binding. Also, through its inclusion, ETMS blocks sites on the glass substrate otherwise available for unwanted protein binding. The optimum condition to produce consistent binding was found to be a total silane concentration of 1.13 mM (APTMS/ETMS in a 1:4 ratio). The samples were then subjected to gold colloid solution as described previously. Variations on the APTMS/ETMS ratio can be seen in Fig. 1, showing the decline in gold population when APTMS was less than 1:4 and rendering the resonance S/N too low to be used. These conditions of preparing the glass substrates with gold colloid were subsequently used in all sensing experiments and the density was calculated as ca. 3.3 colloid particles/μm^2 (Fig. 1a).

The effect of changing the time of incubation of gold colloid with the mixed silane glass substrate was also investigated. The incubation time of a 20-μL drop of colloid in contact with the substrate modified with 1.13 mM APTMS/ETMS (1:4) was observed in 10-min intervals up to and including 40 min. The results can be seen in Fig. 2, where the binding is shown to increase with time. Times greater than 10 min were considered unusable, due to the close proximity of neighboring gold dots. This effect leads to spectral broadening and poorer resolution.

Optical characterization of binding events

In order to assess the sensitivity of our LSPR sensor, we measured the shift in its extinction spectrum induced by the molecular binding occurring at the gold surface. The extinction was measured using a dark-field microscope coupled to a conventional microspectrometer. Regarding the specificity of our detection system, the probed area of the sensor was an area of about 100×100 μm. A dark-field image representation of a probed area can be seen in Fig. 2a.

Biotin/streptavidin system

The conventional and well-known biotin/streptavidin system was used to validate the feasibility of the LSPR sensor and calibrate our acquisition setup (shown in Electronic supplementary material). This system has been shown to have a high affinity characteristic associated with it and has been used in SPR sensing previously [11–13]. Biotin was bound to the gold colloid (0.2–1 mM) and the shift in wavelength monitored when streptavidin (60 kDa) was added. An overall shift of 7–10 nm was recorded under these conditions (see Electronic supplementary material).

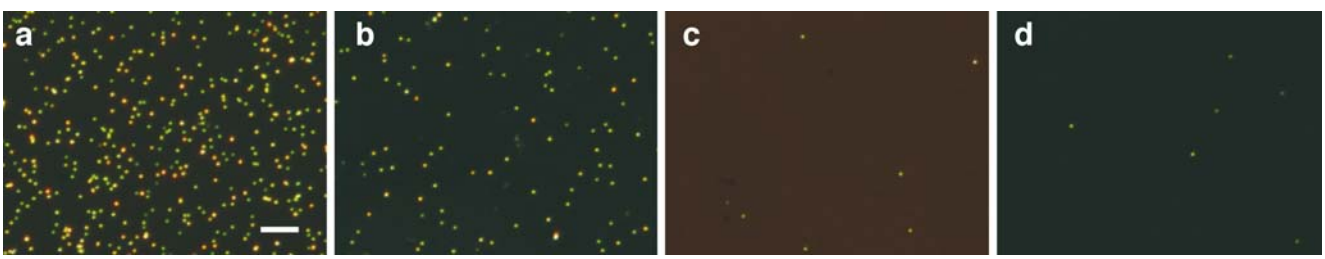

Fig. 1 Dark-field images of gold-modified glass substrates using various ratios of APTMS/ETMS, **a** 1:4, **b** 1:8, **c** 1:16, **d** 1:32. Total silanization was 1.13 mM. *Scale bar* 5 μm

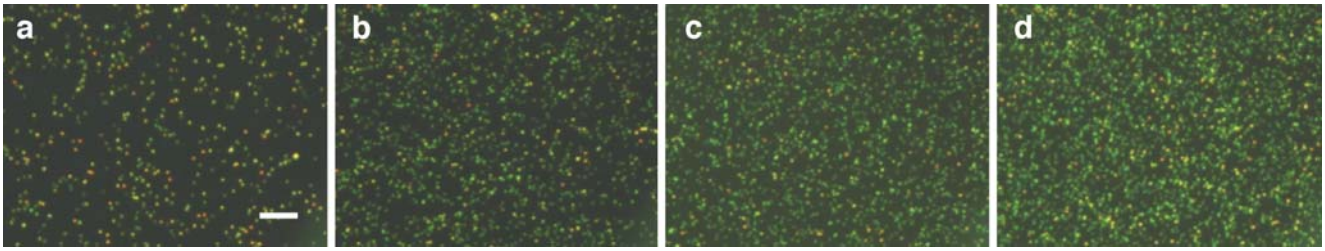

Fig. 2 Dark-field images of the optimization of gold colloid contact time with a 1.13 mM solution APTMS/ETMS (1:4) modified glass substrate for **a** 10 min, **b** 20 min, **c** 30 min, **d** 40 min at RT. *Scale bar* 5 μm

Stanozolol-BSA/α-stanozolol pAb system

Once the LSPR setup was shown to function using biotin/streptavidin, the system utilizing polyclonal serum (pAbs) and the stanozolol coating conjugate (St-BSA) was assessed. The latter has a molecular weight similar to that of streptavidin, whereas the pAbs are immunoglobulins of subtype G (IgG), typically in the 150-kDa range. This should give a measurable wavelength shift when binding firs the coating conjugate (St-BSA) and subsequently recognizing the antibody receptor (α-St pAbs). Affinity of the pAbs vs. the St-BSA was first tested by microplate assay using a noncompetitive ELISA format (data not shown) and the sigmoidal trend observed, based on the law of mass action, was confirmed in the following section.

Optimization of biological reagents

Initial experiments centered on optimizing the coating conjugate (St-BSA) toward the prepared gold-modified glass substrates. A linear response was initially seen when St-BSA increased from 0 to 10 μg/mL (Fig. 3a) with no significant increase in resonance shift noticed at higher concentrations, whilst the maximum resonance shift recorded for St-BSA was 4.2 nm. In order to confirm if this was truly a specific signal, we devised a method to separate the optical transduction mode from the biological binding event. Through the use of an enzyme-labeled anti-species (IgG-HRP), which has a high selectivity for α-St pAbs, we were able to determine the degree of nonspecific binding (NSB) of all the reagents used, to either the silanized glass alone, gold-modified glass, or the protein-coated gold-modified glass. This will be discussed in detail in the next section.

From Fig. 3a, St-BSA at 10 μg/mL was chosen for all future experiments considering that a tenfold increase in concentration did not yield an equivalent shift in resonance wavelength, and thus conserving precious reagent. In a similar fashion, dose-dependent curves were constructed for the binding of the specific receptor, α-St pAb (Fig. 3b). This binding curve was monitored by both the resonance shift of the gold particles and the color emitted when using the secondary labeled anti-species. By choosing both methods it was possible to determine any defects arising from either the resonance or biological binding modes. For the spectrophotometric method, the IgG-HRP was added in a predetermined, nonexcess amount for an additional 30-min incubation period and after an excessive washing step, color was developed as described in the Material and methods. Data have been fitted to a hyperbolic one-site binding equation, using the GraphPad Prism software: $Y=B_{max}X/(K_d + X)$, where B_{max} is the maximum binding and K_d is the concentration of pAb needed to reach half-maximal binding. As can be seen from Fig. 3b, both modes depict an equivalent trend under the conditions used. This suggests that the resonance mode is truly measuring the binding event close to the gold surface. Both curves types are the averaged results on separate days for each method (n=2, N=2). The spectrophotometric result was

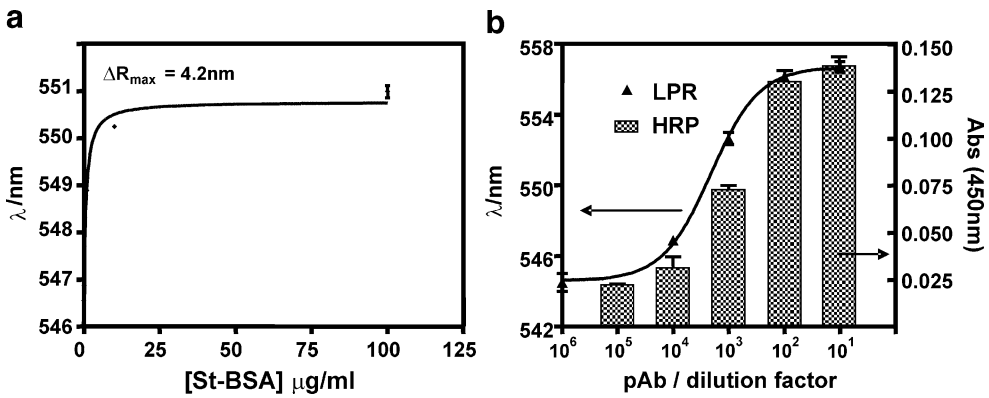

Fig. 3 Dose-dependent curves for the LSPR shift (Δλ), for the binding of **a** St-BSA to bare gold colloid and **b** dilution of α-St pAb stock to gold colloid coated in 10 μg/mL St-BSA (corrected for St-BSA response as determined in part **a**) in resonance (▲) and the spectrophotometric mode (*bar graph*)

also corrected for any background NSB, by inclusion of precise controls (discussed in detail in the following section). Both curves show excellent data fit to the one-site binding equation, of 0.993 or better. Considering both modes, a dilution of α-St pAbs to be used in all future experiments was kept at 1/100 (10^2). We are near saturation of the binding at this value and no gain in terms of resonance shift was seen at higher concentrations. The maximum change in wavelength here was noted at 13.2 nm.

Determination of nonspecific binding

The LSPR setup accounts for binding events in the distinct environment of the resonator, i.e., the gold particle and changes in the dielectric constant close to its surface. As with any system it is paramount to investigate if the overall signal has, in any way, a nonspecific contribution. Therefore it was important to determine if any of the proteins involved in the LSPR biosensor were contributing in such a nonspecific way to the overall signal. As mentioned earlier, this concept was measured in both resonance and spectrophotometric modes. The latter, using a secondary labeled anti-species, was attempted to distinguish between transduction (resonance) and biological modes, insofar as the spectrophotometric mode does not rely on any form of resonance and solely on the judicial binding of the reagents to their targets. This confirmatory method was used in all experiments involving biological reagents, i.e., concentration optimization of St-BSA and α-St pAbs, nonspecific binding profiles, and also in the quantitative determination of St by competitive assay. Within this section, the NSB of the α-St pAbs to silanized glass (Fig. 4, part D1) and to atrazine-BSA (Fig. 4, part B1) and BSA-coated gold colloid (Fig. 4, part C1) was monitored.

In the NSB case of B1 in Fig. 4, we used the same carrier protein (BSA) but different analyte, namely atrazine, to make a coating carrier (At-BSA). In this way the α-St pAbs should not be specific for the atrazine but would see the carrier, BSA, exactly the same as in the specific binding case. This is as close to the specific binding case (A1) as possible with only the analyte as the difference. In this instance, there could be binding of the pAbs or constituents of the serum to either the BSA or any Au particle surface still exposed, which would constitute NSB. However, it is unlikely that NSB to Au would occur as we used a coating concentration that accounted for 90% of maximum signal (saturation) as noted from Fig. 3a. As an additional control, we also included a blank (C1), which consisted of coating the Au colloid with a solution of BSA alone (0.01% w/v or 100 μg/mL). Technically this is not representative of what the α-St pAbs see when approaching the Au particles, as in the specific case, but it gave an idea of the degree of NSB of the serum constituents to BSA alone. Typically, this is routinely tested in standard ELISA methods and, more often than not, NSB of serum to BSA is minimal.

In all cases (A–D) the degree of NSB is denoted by the difference in value between a particular letter, i.e., B1−B2, where B2 is the NSB contribution from the anti-species IgG-HRP and B1 is the combined contribution from IgG-HRP and α-St pAbs. The difference indirectly gives the NSB of the α-St pAbs to At-BSA for the B case, or to BSA for case C and finally for the contribution to silanized glass alone (D). Monitoring the NSB through the spectrophotometric method and thus using the secondary labeled anti-species, it was found that all the NSB accounted for during these measurements came solely from this anti-species. This was deduced from the fact that if you compare values

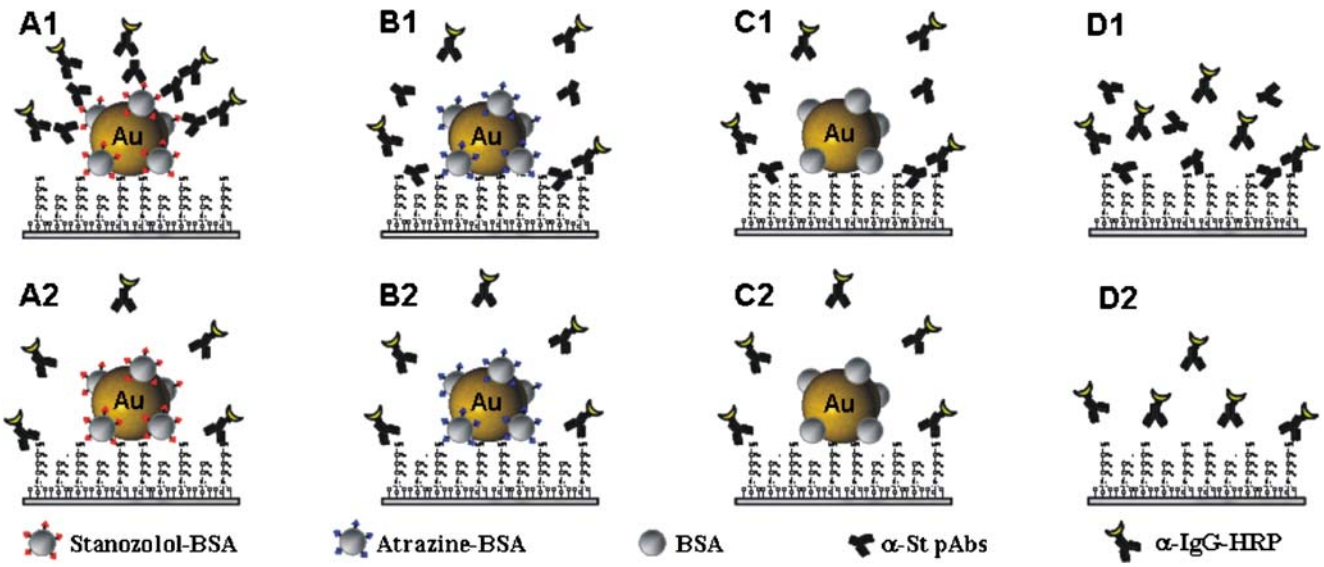

Fig. 4 Schematic of the nonspecific binding controls (*B*, *C*, *D*) used during spectrophotometric experiments on gold colloid bound to glass substrate; *A1* is the specific binding case. Substrates prepared as described in Fig. 1

Table 1 Nonspecific binding controls used for spectrophotometric tests (A2–D2) on gold colloid bound to glass substrate and A1 is specific binding

Control type	A1[a]	A2	B1	B2	C1	C2	D1	D2
Abs (A.U.)	0.371	0.298	0.280	0.281	0.265	0.269	0.212	0.213
CV	0.014	0.004	0.005	0.008	0.010	0.005	0.008	0.013
RSD (%)	3.7	1.3	1.9	3.0	3.6	1.8	3.7	5.9

[a] Absorbance values measured at 450 nm (n=4)

for the same NSB system they are equal considering the error (CV) for these measurements.

In more detail, comparing controls D1 and D2 (Table 1), where the NSB of the pAbs (α-St pAbs and anti-species IgG HRP) was monitored for the silanized glass substrate, it can be seen that no difference in the absorbance values was noted, 0.212 vs. 0.213 A.U., respectively, and therefore no contribution to NSB was apportioned to the α-St pAbs. This concluded that if there was any NSB portion in the specific signal case (A1), it could only derive from a binding of the α-St pAbs to the BSA portion of the carrier. Therefore, by comparing controls C1 and C2, where the gold bound to glass substrate had only a BSA coating, again no contribution was from the α-St pAbs (0.265 vs. 0.269 A.U.). However, in the presence of gold particles coated with BSA, higher absolute NSB was seen (compare to D1). This was further confirmed (controls B1 and B2) when we used the atrazine-BSA to coat the gold and measure the same thing. In this case absorbance values increased slightly (up to 0.280 A.U.) but any NSB contribution was still solely from the secondary anti-species binding to the silanized glass (D1) plus the portion to the atrazine-BSA (0.280 vs. 0.281 A.U.). Therefore, whenever we used the anti-species for spectrophotometric experiments, controls had to be incorporated and subsequently the data treated for this NSB contribution. In those experiments, such as optimization studies and quantitative determination of St, this background value was always subtracted to yield the absorbance results shown in Figs. 3b and 5.

In terms of the LSPR sensor, which did not use IgG-HRP as part of its detection, we now know that there was little, if any, NSB occurring when we measured the specific binding case, as depicted in A1. The α-St pAbs neither bound to the silanized glass substrate nor to BSA or atrazine-BSA-coated gold particles. LSPR experiments were also devised to confirm this NSB phenomenon, with particular focus on the atrazine-BSA case. When used as a substitute for the St-BSA, under identical conditions (concentration and time of incubation), the α-St pAbs did not bind to any significant portion, accounting for <3% of the specific signal (0.4-nm resonance shift) and considering that this is within the error of the measurement, both LSPR and spectrophotometric analysis confirmed that the proteins of choice and the chemistry used to prepare the surface contribute to the high specificity seen in the sensor.

Quantitative determination of stanozolol

Considering the results from both the optimization and the nonspecific binding studies, stanozolol was determined in buffered solutions. In order to quantitate this analyte, we used a preincubation step, as described in Biological modification of gold colloid. Controls were also included, which constituted zero analyte (max signal) and also zero pAb (min signal). The LSPR data returned was fitted to the sigmoidal, variable slope, nonlinear regression equation from the GraphPad Prism software.

In the case of LSPR, the result shown in Fig. 5 was the averaged result over three individual experiments on separate days (N=3). Data have been normalized to account for any day-to-day variations in the control values but resonance signals were of the order of those shown during the optimization steps ($\Delta\lambda_{max}$=10±2 nm). To confirm the LSPR result, the same system, under the same conditions, was also measured by the spectrophotometric method previously described. In this case, we can see that the trend was very similar when fitted to the nonlinear equation. The Hillslope, which gives a measure of the sensitivity of the assay, is measured by a tangent through the point of inflection of the sigmoid (EC_{50}). Values of Hillslope close to 1 are

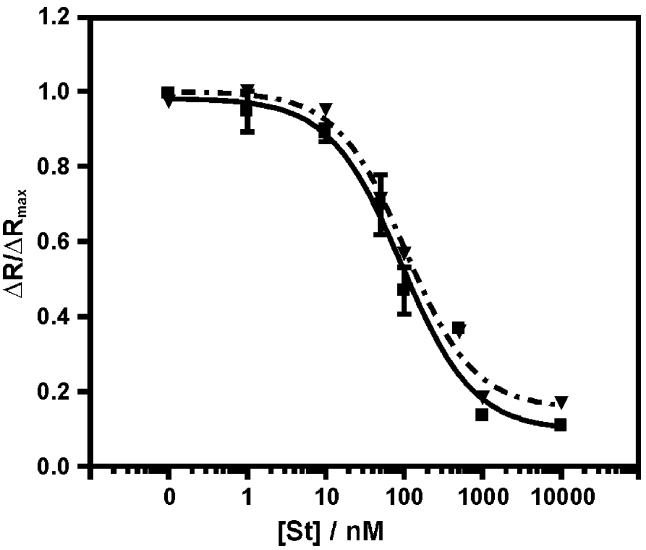

Fig. 5 Quantitation of stanozolol via a preincubation step using gold-colloid-coated glass substrates by two modes, (■) LSPR and (▼) spectrophotometric

considered optimum because of the relationship shown in the equation below. Determination of limit of detection also uses this parameter and thus is an important characteristic of any curve as a deviation from a value of 1 attributes to a less sensitive assay based on the following equation:

$$\mathrm{LOD} = \mathrm{EC}_{50}\left(\frac{\mathrm{Max}-\mathrm{Min}}{\mathrm{Max}-\mathrm{Min}-3\mathrm{SD}_{\mathrm{max}}}-1\right)^{-\frac{1}{k}}$$

Best fit values of Hillslope for both systems in Fig. 5 were found to be −0.9453 and −0.9954. Corresponding EC_{50} values, the concentration of St that caused 50% of the maximum inhibition value and thus the point of the curve considered to be most accurately determined, were 92 and 103 nM. The regression (R^2) values of the fitted curves were 0.968 and 0.991, with the former slightly lower due to one erroneous point in the curve. However, the fitting is still good. Reproducibility of measurement was calculated by averaging the RSD over every point of the curve and values were found to be <5% for separate assays on separate days (n=3, N=3). The detection limit of the system was calculated as 2.4 nM or 0.7 μg/L St, a value below the minimum required performance level (MRPL) used by the International Olympic Committee (IOC) for banned substances, determined by chromatographic methods [14–15]. This detection level is considered close to modern SPR analysis [16–17] and suitable for measuring analytes of this size and nature [18–20]. In terms of sensitivity to other reported colloidal-based systems, it is at least an order of magnitude lower than these, with detection limits reported between 1,000 and 30 nM [5, 21–22].

Conclusion

When you compare this method to both conventional SPR and chromatographic techniques, the latter require skilled personnel, preconjugation of targets for column analysis, and expensive equipment, not to mention the time of analysis associated with the preparation of standard calibration curves and sample detection. With this LSPR method measurement time of these standards and of an unknown sample (n=18), it is feasible to contemplate a total time of <80 min, i.e., each sample taking ca. 2 min to determine. Therefore we can consider the method as a relatively fast and cheaper alternative for the analytical determination of steroid hormones.

Acknowledgments This work was supported by the Spanish Ministry of Science and Technology (TIC2003-01038 & AGL2005-07700-C06-01 & DEP2007-73224-C03-00) and by the European Commission (IST-2003-508774 & NMP2-CT-2003-505485) and the Regional Development Fund. MPK thanks the Ministerio de Educación, Cultura y Deporte for his fellowship under the National Program of Mobility for Professors and Researchers. The AMR group is a Grup de Recerca de la Generalitat de Catalunya and has support from the Departament d'Universitats, Recerca i Societat de la Informació la Generalitat de Catalunya (expedient 2005SGR 00207).

References

1. Gu JH, Lu H, Chen YW, Liu LY, Wang P, Ma JM, Lu ZH (1998) Supramol Sci 5:695–698
2. He L, Musick MD, Nicewarner SR, Salinas FG, Benkovic SJ, Natan MJ, Keating CD (2000) J Am Chem Soc 122:9071–9077
3. He L, Smith EA, Natan MJ, Keating CD (2004) J Phys Chem B 108:10973–10980
4. Lyon LA, Musick MD, Natan MJ (1998) Anal Chem 70:5177–5183
5. Lyon LA, Musick MD, Smith PC, Reiss BD, Peña DJ, Natan MJ (1999) Sens Actuators B 54:118–124
6. Riboh JC, Haes AJ, McFarland AD, Yonzon CR, Van Duyne RP (2003) J Phys Chem B 107:1772–1780
7. Enoch S, Quidant R, Badenes G (2004) Opt Express 12:3422–3427
8. Rechberger W, Hohenau A, Leitner A, Krenn JR, Lamprecht B, Aussenegg FR (2003) Opt Comms 220:137–141
9. Gascón J, Oubiña A, Ballesteros B, Barceló D, Camps F, Marco M-P, Angel González-Martínez M, Morais S, Puchades R, Maquieira A (1997) Anal Chim Acta 347:149–162
10. Tätte T, Saal K, Kink I, Kurg A, Lõhmus R, Mäeorg U, Rahi M, Rinken A, Lõhmus A (2003) Surf Sci 532–535:1085–1091
11. Malmqvist M (1993) Nature 361:186–187
12. Jordan CE, Frutos AG, Thiel AJ, Corn RM (1997) Anal Chem 69:4939–4947
13. Kalyuzhny G, Vaskevich A, Schneeweiss MA, Rubinstein I (2002) Chem Eur J 8:3849
14. Schänzer W, Donike M (1993) Anal Chim Acta 275(1–2):23–48
15. Merode A (1998) IOC guidelines, vol 8. IOC, Lausanne
16. Soh N, Tokuda T, Watanabe T, Mishima K, Imato T, Masadome T, Asano Y, Okutani S, Niwa O, Brown S (2003) Talanta 60:733–745
17. Cui X, Yang F, Sha Y, Yang X (2003) Talanta 60:53–61
18. Ehrentreich-Förster E, Scheller FW, Bier FF (2003) Biosens Bioelectron 18:375–380
19. Akkoyun A, Kohen VF, Bilitewski U (2000) Sens Actuators B 70:12–18
20. Gillis EH, Gosling JP, Sreenan JM, Kane M (2002) J Immun Methods 267:131–138
21. Raschke G, Kowarik S, Franzl T, Sönnichsen C, Klar TA, Feldmann J, Nichtl A, Kurzinger K (2003) Nano Letts 3:935–938
22. Frederix F, Friedt JM, Choi KH, Laureyn W, Campitelli A, Mondelaers D, Maes G, Borghs G (2003) Anal Chem 75:6894–6900